Frontiers in Life Sciences and Related Technologies 3(3) (2022) 95-100

Contents lists available at Dergipark

Frontiers in Life Sciences and Related Technologies

Journal homepage: http://dergipark.org.tr/en/pub/flsrt

Research article

Long-range transport and potential source regions of $PM_{2.5}$ during the autumn season in Edirne, Türkiye

Ilker Oruc*[1]

[1] Kirklareli University, Vocational College of Technical Sciences, 39010, Kirklareli, Türkiye

Abstract

The variation in daily Particulate Matter 2.5 ($PM_{2.5}$) concentrations was studied in Edirne city center from September 1, 2019 to November 30, 2019 (autumn season). The values of daily $PM_{2.5}$ concentrations were between 5.65 and 77.59 µg m^{-3}. The values of $PM_{2.5}$ concentration had the highest average value on Tuesdays compared to other days. The mean value of daily $PM_{2.5}$ concentrations on Tuesdays was 23.41 µg m^{-3}. The backward trajectories were computed and clustered by applying the Hybrid Single-Particle Lagrangian Integrated Trajectory (HYSPLIT) model. The backward trajectories clustered in eight major clusters during the autumn. In Cluster 4 (C4), which has more short-range transport according to the other seven clusters, the mean value of $PM_{2.5}$ concentrations was 19.52 µg m^{-3}. The mean value of $PM_{2.5}$ concentrations was 28.11 µg m^{-3} in C8 (3.3%), which has more long-range transport than the other seven clusters. Potential source areas of $PM_{2.5}$ have been determined by the Potential Source Contribution Function (PSCF) model. The results of PSCF analyses illustrated that the north, northeast, south, and southeast regions of the sampling area as major potential source areas for $PM_{2.5}$. The results obtained in this study can make important contributions to the evaluation of $PM_{2.5}$ concentration in the region in terms of health and long-range transport.

Keywords: *Backward trajectory; HYSPLIT; particulate matter; $PM_{2.5}$; PSCF*

1. Introduction

Due to their properties and weather conditions, pollutants released into the atmosphere can be transported long distances from emission sources (Lagzi et al., 2013; Ozdemir et al., 2021). It has been described that when aerosols are generated by gas-to-particle conversion, long-distance transport is possible because the duration needed for gas-to-particle conversion and the relatively small particle sizes produced by this process result in long residence times in the atmosphere (Wallace and Hobbs, 2006; Flores et al., 2020). Various air pollutants released into the atmosphere can be cited as the cause of many current and potential environmental problems (Lagzi et al., 2013). Air pollution in cities is very complex due to many emission sources, meteorological processes, and chemical transformations (Ho, 2012). Because of the large number of anthropogenic emission sources in urban and industrialized locations, the concentrations of various undesirable pollutants can cause deterioration of air quality and visibility and reach levels that threaten human health (Wallace and Hobbs, 2006). In a study carried out by Hao et al. (2019), it was stated that the southerly route represents the main transport route of $PM_{2.5}$ for all seasons. It was noted that the northwesterly transport route passes through the natural source areas, while the southerly transport route passes through the anthropogenic source areas. The percentage of pollution trajectories in each cluster (C1, C2, C3, C4, C5, C6) during the autumn season was 71.40%, 9.30%, 32.00%, 24.30%, 60.10%, 10.60%, respectively. The mean values of $PM_{2.5}$ concentrations were 142, 144, 119, 144, 129, and 117 µg m^{-3} in these clusters. The study by Cheng et al. (2017) noted that the percentage of all trajectories during the autumn season was 12.71% in C1, 3.84% in C2, 11.10% in C3, 18.23% in C4, 31.01% in C5, 13.69% in

* Corresponding author.
E-mail address: ilkeroruc@klu.edu.tr (I. Oruc).
https://doi.org/10.51753/flsrt.1113251 Author contributions
Received 09 May 2022; Accepted 20 September 2022
Available online 20 October 2022

C6, 0.84% in C7, 6.84% in C8, and 1.75% in C9. They explained that mean values of $PM_{2.5}$ concentrations in these clusters were 73.12, 41.52, 69.93, 37.71, 50.24, 34.41, 44.97, 28.85, 60.64 µg m^{-3}, respectively. In the study performed by Zhao et al. (2015), the mean values of $PM_{2.5}$ concentration in C1, C2, C3, C4, and C5 during the autumn season were 63.14, 78.47, 119.94, 95.96, and 38.34 µg m^{-3}, respectively. Li et al. (2020) stated that the distribution of air masses in the autumn season is similar to that in the spring and winter seasons. In their study, the mean values of $PM_{2.5}$ concentrations in C1, C2, C3, C4, C5, and C6 during the autumn season were 8.79, 7.25, 9.88, 7.32, 8.75, and 9.76 µg m^{-3}, respectively. They explained that the percentage of all trajectories in these clusters were 14.3%, 29.7%, 16.2%, 7.6%, 25.4%, 6.8%, respectively. Cluster analysis performed by Li et al. (2017) indicated that Beijing in autumn was influenced by trajectories from both the south and southeast. The percentage of all trajectories during the autumn was 16.76% in C1, 36.08% in C2, 13.32% in C3, 12.77% in C4, 5.72% in C5, and 15.34% in C6. The mean values of $PM_{2.5}$ concentrations in these clusters during the autumn were 94.19, 41.64, 169.78, 46.56, 91.59, and 165.17 µg m^{-3}, respectively. In the study of Lv et al. (2021), the number of trajectories was 2160 in autumn. It was stated that in the autumn, other clusters except for C5 gathered trajectories from the north, and these trajectories represented 91.90% of all trajectories. The percentage of trajectory numbers of each cluster in all trajectories during the autumn season was 41.02% in C1, 24.91% in C2, 14.77% in C3, 11.20% in C4, and 8.10% in C5. The average values of $PM_{2.5}$ concentration in these clusters were 38.35, 33.27, 34.06, 25.38, and 63.83 µg m^{-3}, respectively.

In many studies, the PSCF approach has been performed to identify potential source areas of $PM_{2.5}$ (Wang et al., 2015; Cheng et al., 2017; Mukherjee and Agrawal, 2018; Li et al., 2020). It was stated by Wang et al. (2015) that the regional emission source's probable locations during relatively polluted periods are mainly south and west of Beijing. It was explained that the $PM_{2.5}$ sources are primarily areas on the regional scale owing to the long-distance transport tendency. Cheng et al. (2017) stated that the potential source areas of $PM_{2.5}$ extend further northward in autumn, but the transport routes are the same as in the spring. External $PM_{2.5}$ source areas were reported to be mainly located in the southeast and northwest in autumn. The study by Li et al. (2020) noted that in the northern part of Xinjiang are concentrated severe pollution source areas of $PM_{2.5}$ in autumn. According to the PSCF results in the study of Mukherjee and Agrawal (2018), the northwest has been defined as the main source area with a higher possibility of contributing to the higher fine particulate matter load in Varanasi city. Further, they stated that there are other possible sources from the east and north directions. They also stated that the contribution probability of the sources coming from the east direction is the lowest. Li et al. (2017) stated that their study's potential source areas of PM_{10} and $PM_{2.5}$ are similar according to the concentration weighted trajectory (CWT) and PSCF results. Wu et al. (2018) explained that according to the PSCF analysis performed in their study, the main reason for the high $PM_{2.5}$ levels detected in northern Henan could be extraneous polluted air masses.

In this study, daily $PM_{2.5}$ concentrations in the Edirne city center during the autumn season (between September 1, 2019, and November 30, 2019) have been studied. The backward trajectories have been run and clustered by applying the HYSPLIT Model. Transport pathways and potential source areas of $PM_{2.5}$ have been determined.

2. Materials and methods

2.1. Sampling location

Edirne Province is located between 41º 40' North latitude and 26º 30' East longitude (Fig. 1). Edirne Province is a border city neighboring Greece to the west and Bulgaria to the north. In addition, Kirklareli and Tekirdag Provinces are located to the east of Edirne Province, and Canakkale Province to the south. Certain parts of the Meric, Tunca, Arda, and Ergene rivers are located within the borders of Edirne Province. The continental climate is dominant in Edirne Province (ECDR, 2020). Daily $PM_{2.5}$ concentrations obtained from the Air Quality Monitoring Station in Edirne city center were used (MEUCC, 2022).

2.2. Backward trajectories analysis

In this study, to define the origins and transport pathways of air masses reaching the study point the HYSPLIT model was used. The backward trajectories were computed and clustered at 1-hour intervals for 72 hours and at an arrival height of 1500 meters above the ground. The weekly stored data consisting of 1º resolution outputs of the Global Data Analysis System (GDAS) were used as input (Stein et al., 2015; Rolph et al., 2017). The Euclidean distance used for clustering backward trajectories is presented below (Carslaw and Ropkins, 2012; Carslaw, 2019).

$$d_{1,2} = \left(\sum_{i=1}^{n} ((X_{1i} - X_{2i})^2 + (Y_{1i} - Y_{2i}))^2 \right)^{1/2}$$
(Equation 1)

In the equation, X_1, Y_1 and X_2, Y_2 are coordinates (the latitude and longitude) of the backward trajectories 1 and 2, respectively. n is the number of backward trajectories points.

2.3. PSCF analysis

The PSCF approach is a widely used method to identify possible source areas of pollutants (Begum et al. 2005; Pekney et al., 2006; Carslaw and Ropkins, 2012; Li et al. 2017; Kuzu and Saral, 2017; Carslaw, 2019; Neykova and Hristova, 2020; Oruc, 2022). PSCF solves

$$PSCF_{ij} = \frac{m_{ij}}{n_{ij}}$$
(Equation 2)

In the equation, while the number of trajectories passing in the ij^{th} grid cell is defined as n_{ij}, the number of times a source concentration is high than a given value of criterion when trajectories pass in the ij^{th} grid cell was defined as m_{ij}. The value of the criterion was specified as 75% of all samples (Jain et al., 2017; Bie et al., 2021; Oruc, 2022). PSCF scores were multiplied by weighting values. The weight values ($W(n_{ij})$) given in the equation below are used (Petroselli et al., 2018; Oruc, 2022).

In the equation, $\overline{n}$ represents the mean number of endpoints per cell, which is calculated on every cell with at least one end-

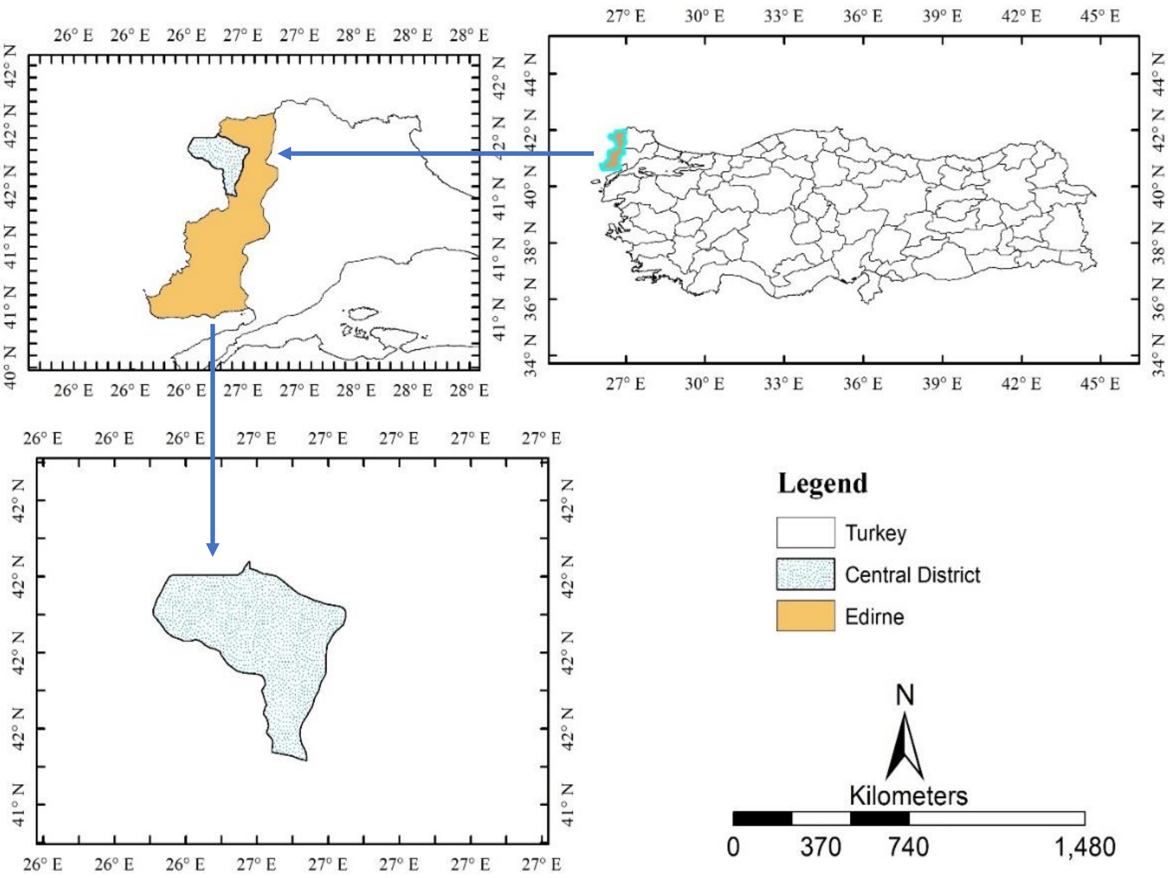

Fig. 1. Sampling location.

point. The figures in this study were created by applying the OpenAir statistical analysis package with the R-Studio program (Carslaw and Ropkins, 2012; Carslaw, 2019).

$$W(n_{ij}) = \begin{cases} 1.00, n_{ij} > 2\bar{n} \\ 0.75, \bar{n} < n_{ij} \leq 2\bar{n} \\ 0.50, \bar{n}/2 < n_{ij} \leq \bar{n} \\ 0.15, n_{ij} \leq \bar{n}/2 \end{cases}$$

(Equation 3)

3. Results and discussion

The mean value of daily $PM_{2.5}$ concentrations measured during the study period was 20.40 µg m^{-3}. The values of $PM_{2.5}$ are relatively higher in October compared to September and November (Fig. 2). The $PM_{2.5}$ concentrations had the highest daily values on October 29 (77.59 µg m^{-3}) and, the lowest (5.65 µg m^{-3}) on September 11. The maximum concentration of $PM_{2.5}$ was 25.02 µg m^{-3} in September. The minimum value for October was 6.08 µg m^{-3}. The mean values of $PM_{2.5}$ concentrations were 10.61, 27.39, and 22.12 µg m^{-3} in September, October, and November, respectively. The $PM_{2.5}$ concentrations were between 7.09 and 43.57 µg m^{-3} in November.

The results shown on Fig. 3 demonstrate the variations in the mean $PM_{2.5}$ concentrations among the weekdays. The shading expresses the 95% confidence intervals of the mean $PM_{2.5}$ concentration values. The mean values of $PM_{2.5}$ concentrations were 22.81, 20.30, 21.91, 19.04, and 18.10 µg m^{-3} on Mondays, Wednesdays, Thursdays, Saturdays, and Sundays, respectively. The minimum values of $PM_{2.5}$ concentrations were 5.92, 7.00, 5.65, 6.62, 5.99, 6.08, and 6.64 µg m^{-3} on Mondays, Tuesdays, Wednesdays, Thursdays, Fridays, Saturdays, and Sundays, respectively. The maximum values of $PM_{2.5}$ concentrations were 50.62, 77.59, 43.57, 51.86, 45.95, 49.00, and 47.19 µg m^{-3} on these days, respectively. The values obtained during the study draw the trend of observing the highest values of $PM_{2.5}$ on Tuesdays (23.41 µg m^{-3}) and the lowest concentrations on Fridays (17.42 µg m^{-3}).

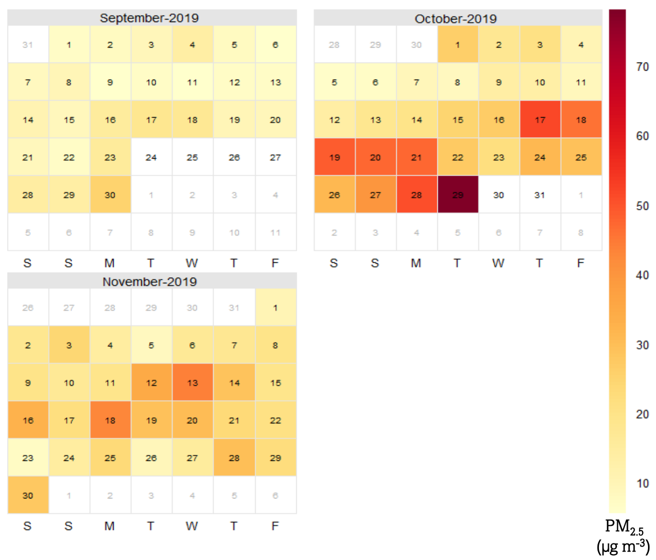

Fig. 2. CalendarPlot of $PM_{2.5}$ concentrations during the autumn in 2019.

The backward trajectories are clustered in an 8-cluster solution (Fig. 4). Trajectories within C1 accounted for 11% of all trajectories. The values of $PM_{2.5}$ concentrations were seen to range between 5.65 and 31.22 µg m^{-3} in C1. Among the clusters, the average value of $PM_{2.5}$ concentrations was the lowest in C1 (13.76 µg m^{-3}). The transport in C1 originated from Russia. It was seen that arrived at the sampling area by passing over the Sea of Azov, Ukraine, the Black Sea, and Bulgaria. Trajectories within both C2 and C7 accounted for 14.3% of all trajectories. In C2, the mean value of $PM_{2.5}$ concentrations was 20.46 µg m^{-3}. It was observed that $PM_{2.5}$ concentration values in C2 ranged between 5.99 and 47.03 µg m^{-3}. The transport in C2 started from Ukraine. It was seen that arrived at the sampling area via the Black Sea and Bulgaria. The values of $PM_{2.5}$ concentrations in C7 ranged between 10.02 and 42.59 µg m^{-3}, with a mean value of 26.78 µg m^{-3}.

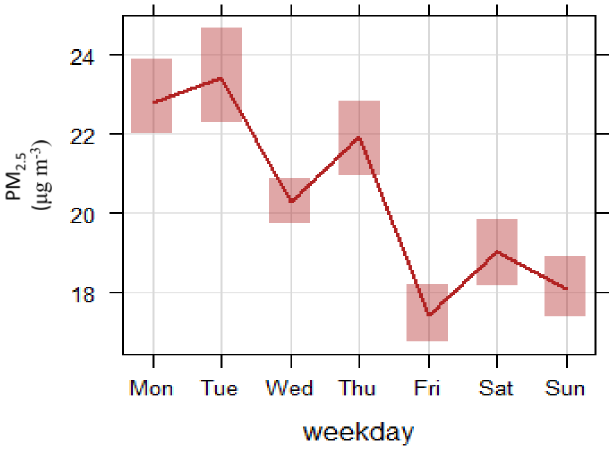

Fig. 3. The mean $PM_{2.5}$ concentrations on weekday.

The transport in C7 originated from the Mediterranean and reached the sampling area by passing over Turkey's Mediterranean, Aegean, and Marmara Regions. It was observed that C3 (17.6%) originated from the Nederland-German land border region. The values of $PM_{2.5}$ in C3 were 8.76 and 50.62 µg m^{-3}, with a mean value of 20.08 µg m^{-3}. The percentage of all trajectories during the study period was higher in C4 (20.9%) compared to the other seven clusters. The mean value of $PM_{2.5}$ concentrations in C4 was 19.52 µg m^{-3}. The values of $PM_{2.5}$ were between 6.08 and 77.59 µg m^{-3} in C4. It was seen that C4, which has short-range trajectories according to other clusters, originated from Bulgaria.

The study by Ecer et al. (2017) stated that backward trajectories were grouped in 6 main clusters during the data collection period. They suggested that the transport in these clusters originates from Syria (C1), France and Southern Europe (C2), Eastern Anatolia (C3), Mediterranean (C4), Middle East (C5), and Central-Western Europe (C6). The percentage of all trajectories in these clusters was 31.1%, 12.2%, 16.9%, 20.1%, 9.3%, and 10.3%, respectively. Zeydan and Wang (2019) stated the backward trajectories during the study period were clustered in 9 main clusters. C1 was noted to originate from the southeast of the United Kingdom and C4 was noted to transport Saharan dust to the sampling area. Tepe and Dogan (2021) pointed out that the backward trajectories in the period of their study were gathered in 5 main clusters. These clusters are named C1 as Northern Europe, C2 as Central Europe, C3 as Anatolia, and the Middle East, C4 as North Africa and Western Mediterranean, and C5 as Levant Region and the Aegean Sea. They stated that the highest percentage of trajectories from C3 with 41%, followed by C5 (23%) and C4 (15%).

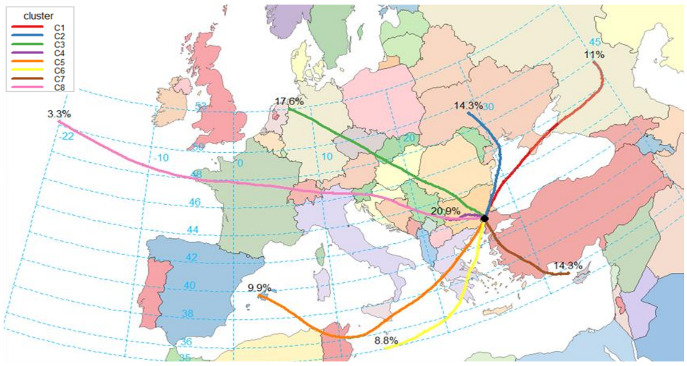

Fig. 4. Backward trajectory clusters.

The values of $PM_{2.5}$ concentrations in C5 were between 6.88 and 51.86 µg m^{-3}, with a mean value of 19.58 µg m^{-3}. The transport in C5 originated from the west coasts of Majorca Island. It was seen that reached the sampling area by passing over the Mediterranean, Algeria, Tunisia, Italy, Greece, and Bulgaria. It was observed that trajectories within C5 and C6 accounted for 9.9% and 8.8% of all trajectories, respectively. The values of $PM_{2.5}$ concentration were between 10.61 and 49.00 µg m^{-3} in C6, while the mean value is 20.87 µg m^{-3}.

It was observed that C6, which originated from the Mediterranean, arrived at the sampling area via Greece and the Aegean Sea. The percentage of all trajectories during the study period was lower in C8 (3.3%) compared to the other seven clusters. C8 had more long-range transport than the other seven clusters. The values of $PM_{2.5}$ concentration were observed to range between 20.72 and 43.57 µg m^{-3} in C8. Among the clusters, the average value of $PM_{2.5}$ concentrations was the highest in C8 (28.11 µg m^{-3}). The transport in C8 originated from the North Atlantic Ocean.

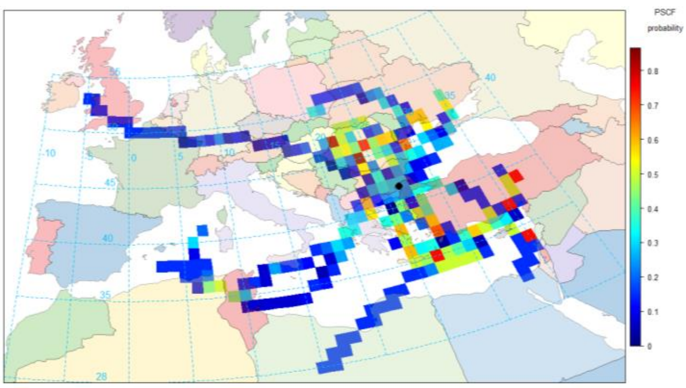

Fig. 5. PSCF distribution of $PM_{2.5}$.

PSCF analysis was carried out to enable the determination of possible potential $PM_{2.5}$ source areas. PSCF distribution illustrated the sampling area's north, northeast, south, and southeast regions as the major potential source areas for $PM_{2.5}$ (Fig. 5).

The higher PSCF values were seen in Romania, Hungary, Turkey, the Mediterranean, and Lebanon than in other locations. In the study carried out by Kuzu and Saral (2017), they explained that trajectories over the Sea of Marmara had the highest PSCF scores on each of the particle sizes. They stated that this confirmed the contribution of marine aerosols. They also explained that sizes of particles between 7.2-3 and 3-1.5 µm, in addition to the marine aerosol contribution, appear to have originated from the crust from the south of Istanbul.

4. Conclusion

The mean value of daily $PM_{2.5}$ concentrations was 20.40 μg m^{-3} in Edirne city center during the autumn season. The lowest and highest values of daily $PM_{2.5}$ concentrations ranged between 5.65 and 77.59 μg m^{-3}, respectively.

The values of $PM_{2.5}$ concentration had the highest average value on Tuesdays compared to other days, with a mean of 23.41 μg m^{-3}. The mean values of daily $PM_{2.5}$ concentration had the lowest daily mean value on Fridays (lowest days), Saturdays, and Sundays to other days. The mean values of daily $PM_{2.5}$ concentrations these days were 17.42, 19.04, and 18.10 μg m^{-3}, respectively. It was determined that the percentage of all backward trajectories of each cluster represented 11% in C1, 14.3% in C2, 17.6% in C3, 20.9% in C4, 9.9% in C5, 8.8% in C6, 14.3% in C7, and 3.3% in C8, respectively. The mean values of $PM_{2.5}$ concentrations were 13.76, 20.46, 20.08, 19.52, 19.58, 20.87, 26.78, and 28.11 μg m^{-3} at these clusters, respectively.

The results of the PSCF analyses indicated that the major potential source areas of $PM_{2.5}$ are especially Romania, Hungary, Turkey, the Mediterranean, and Lebanon.

Conflict of interest: The author declares that he has no conflict of interests.

Informed consent: The author declares that this manuscript did not involve human or animal participants and informed consent was not collected.

References

Begum, B. A., Kim, E., Jeong, C. H., Lee, D. W., & Hopke, P. K. (2005). Evaluation of the potential source contribution function using the 2002 Quebec forest fire episode. *Atmospheric Environment*, *39*(20), 3719-3724.

Bie, S., Yang, L., Zhang, Y., Huang, Q., Li, J., Zhao, T., ... & Wang, W. (2021). Source appointment of $PM_{2.5}$ in Qingdao port, east of China. *Science of the Total Environment*, *755*, 142456.

Carslaw, D. C., & Ropkins, K. (2012). Openair-An R package for air quality data analysis. *Environmental Modelling & Software*, *27-28*, 52-61.

Carslaw, D. C. (2019). *The openair manual - open-source tools for analysing air pollution data*. Manual for version 2.6-6, University of York.

Cheng, F., Zha, Y., Zhang, J., He, J., & Yan, S. (2017). A study on distance transport of $PM_{2.5}$ to Xianlin in Nanjing, China and its source areas. *Aerosol and Air Quality Research*, *17*(7), 1672-1683.

Ecer, A., Sarikaya, B., Tepe, A. M., & Dogan, G. (2017). Mardin hava kirliliğinin değerlendirilmesi. *VII. Ulusal Hava Kirliliği ve Kontrolü Sempozyumu*, Antalya, Türkiye. 853-862.

ECDR, (2020). Edirne İli 2019 Yılı Çevre Durum Raporu, Türkiye Cumhuriyeti Edirne Valiliği Çevre ve Şehircilik İl Müdürlüğü. https://webdosya.csb.gov.tr/db/edirne/icerikler/2019-yili-ed-rne-il--cevre-durum-raporu-n-ha--20201216122442.pdf, Last accessed on July 30, 2022.

Flores, R. M., Mertoglu, E., Ozdemir, H., Akkoyunlu, B. O., Demir, G., Unal, A., & Tayanc, M. (2020). A high-time resolution study of PM2. 5, organic carbon, and elemental carbon at an urban traffic site in Istanbul. *Atmospheric Environment*, *223*, 117241.

Hao, T., Cai, Z., Chen, S., Han, S., Yao, Q., & Fan, W. (2019). Transport pathways and potential source regions of $PM_{2.5}$ on the west coast of Bohai Bay during 2009-2018. *Atmosphere*, *10*(6), 345.

Ho, B. Q. (2012). Urban air pollution. In: Mukesh Khare (ed) *Air Pollution-Monitoring, Modelling and Health* (pp. 1-38). InTech, Rijeka, Croatia.

Jain, S., Sharma, S. K., Choudhary, N., Masiwal, R., Saxena, M., Sharma, A., ... & Sharma, C. (2017). Chemical characteristics and source apportionment of $PM_{2.5}$ using PCA/APCS, UNMIX, and PMF at an urban site of Delhi, India. *Environmental Science and Pollution Research*, *24*(17), 14637-14656.

Kuzu, S. L., & Saral, A. (2017). The effect of meteorological conditions on aerosol size distribution in Istanbul. *Air Quality, Atmosphere & Health*, *10*, 1029-1038.

Lagzi, I., Mészáros, R., Gelybó, G., & Leelőssy, Á. (2013). *Atmospheric chemistry* (pp. 1-201). Eötvös Lorand University.

Li, D., Liu, J., Zhang, J., Gui, H., Du, P., Yu, T., ... & Cheng, Y. (2017). Identification of long-range transport pathways and potential sources of $PM_{2.5}$ and PM_{10} in Beijing from 2014 to 2015. *Journal of Environmental Sciences*, *56*, 214-229.

Li, H., He, Q., & Liu, X. (2020). Identification of long-range transport pathways and potential source regions of $PM_{2.5}$ and PM_{10} at Akedala Station, Central Asia. *Atmosphere*, *11*(11), 1183.

Lv, M., Hu, A., Chen, J., & Wan, B. (2021). Evolution, transport characteristics, and potential source regions of $PM_{2.5}$ and O_3 pollution in a Coastal City of China during 2015-2020. *Atmosphere*, *12*(10), 1282.

MEUCC, (2022). Air Quality Monitoring Station of Republic of Turkey Ministry of Environment, Urbanization and Climate Change, https://sim.csb.gov.tr/STN/STN_Report/StationDataDownloadNew, Last accessed on July 30, 2022.

Mukherjee, A., & Agrawal, M. (2018). Assessment of local and distant sources of urban $PM_{2.5}$ in middle Indo-Gangetic plain of India using statistical modeling. *Atmospheric Research*, *213*, 275-287.

Neykova, R., & Hristova, E. (2020). Backward trajectories and cluster analyses for study of PM_{10} concentration variations in Bulgarian urban areas. *Bulgarian Journal of Meteorology and Hydrology*, *24*(2), 66-83.

Oruc, I. (2022). Transport routes and potential source areas of PM_{10} in Kirklareli, Turkey. *Environmental Monitoring and Assessment*, *194*(2), 104.

Ozdemir, H., Aktas, M. A., Yalcin, I. E., Alyuz, U., Okten, H. E., Ozcan, H. K., ... & Alper, U. (2021). Noktasal kaynaklar için ulusal hava kirliliği emisyon faktörleri ve envanterinin belirlenmesi: Metal sektörü için örnek bir çalışma. *International Journal of Advances in Engineering and Pure Sciences*, *33*(3), 337-346.

Pekney, N. J., Davidson, C. I., Zhou, L., & Hopke, P. K. (2006). Application of PSCF and CPF to PMF-Modeled sources of $PM_{2.5}$ in Pittsburgh. *Aerosol Science and Technology*, *40*(10), 952-961.

Petroselli, C., Crocchianti, S., Moroni, B., Castellini, S., Selvaggi, R., Nava, S., ... & Cappelletti, D. (2018). Disentangling the major source areas for an intense aerosol advection in the Central Mediterranean on the basis of Potential Source Contribution Function modeling of chemical and size distribution measurements. *Atmospheric Research*, *204*, 67-77.

Rolph, G., Stein, A., & Stunder, B. (2017). Real-time environmental applications and display system: READY. *Environmental Modelling & Software*, *95*, 210-228.

Stein, A. F., Draxler, R. R., Rolph, G. D., Stunder, B. J. B., Cohen, M. D., & Ngan, F. (2015). NOAA's HYSPLIT atmospheric transport and dispersion modeling system. *Bulletin of the American Meteorological Society*, *96*(12), 2059-2077.

Tepe, A. M., & Dogan, G. (2021). Chemical characterization of PM2.5 and PM2.5-10 samples collected in urban site in Mediterranean coast of Turkey. *Atmospheric Pollution Research*, *12*(1), 46-59.

Wallace, J. M., & Hobbs, P. V. (2006). *Atmospheric science an introductory survey (2nd ed.).* (pp. 1-483). Elsevier Inc., San Diego.

Wang, L., Liu, Z., Sun, Y., Ji, D., & Wang, Y. (2015). Long-range transport and regional sources of $PM_{2.5}$ in Beijing based on long-term observations from 2005 to 2010. *Atmospheric Research*, *157*, 37-48.

Wu, X., Ding, Y., Zhou, S., & Tan, Y. (2018). Temporal characteristic and source analysis of $PM_{2.5}$ in the most polluted city agglomeration of China. *Atmospheric Pollution Research*, *9*(6), 1221-1230.

Zeydan, O., & Wang, Y. (2019). Using MODIS derived aerosol optical depth to estimate ground-level $PM_{2.5}$ concentrations over Turkey. *Atmospheric Pollution Research*, *10*(5), 1565-1576.

Zhao, M., Huang, Z., Qiao, T., Zhang, Y., Xiu, G., & Yu, J. (2015). Chemical characterization, the transport pathways and potential sources of $PM_{2.5}$ in Shanghai: Seasonal variations. *Atmospheric Research*, *158-159*, 66-78.

Cite as: Oruc, I. (2022). Long-range transport and potential source regions of $PM_{2.5}$ during the autumn season in Edirne, Türkiye. *Front Life Sci RT, 3*(3), 95-100.